Indian Journal of Chemical Technology
Vol. 25, January 2018, pp. 51-60

Influence of Al_2O_3 nanoparticles on the dielectric properties and structural dynamics of PVA-PEO blend based nanocomposites

Shobhna Choudhary[1,2]

[1]Dielectric Research Laboratory, Department of Physics, Jai Narain Vyas University, Jodhpur 342 005, India
[2]CSIR-National Institute of Science Communication and Information Resources, New Delhi 110 012, India
E-mail: shobhnachoudhary@rediffmail.com

Received 15 August 2017; accepted 15 October 2017

The organic-inorganic nanocomposite films comprising poly(vinyl alcohol) (PVA) and poly(ethylene oxide) (PEO) blend matrix dispersed with alumina (Al_2O_3) nanoparticles (i.e., (PVA-PEO)–*x*wt% Al_2O_3; x = 0, 1, 3 or 5) have been prepared by the solution-cast method. The X-ray diffraction study confirms a large decrease in crystalline phase of the PVA-PEO blend structures with the addition of 1 wt% Al_2O_3, and it decreases gradually with the further increase of Al_2O_3 contents. Influence of Al_2O_3 nanofiller on the complex dielectric permittivity, electrical conductivity, electric modulus and the impedance properties of these polymer nanocomposite (PNC) films have been investigated over the frequency range from 20 Hz to 1 MHz by employing the dielectric relaxation spectroscopy (DRS). The ambient temperature dielectric permittivity values of the PNC films decrease initially up to 3 wt% Al_2O_3 loading in the PVA-PEO blend matrix, whereas for 5 wt% Al_2O_3, it again increases and exceeds the value of pristine polymer blend film.The relaxation processes exhibited in the dielectric loss tangent and the loss part of electric modulus spectra reveal that the polymers cooperative chain segmental motion enhances in the presence of Al_2O_3 nanoparticles in the PVA-PEO blend structures. Further, it has been found that the values of dielectric permittivity increase whereas the relaxation time decreases with the increase of temperature of the (PVA-PEO)–3 wt% Al_2O_3 film from 27 to 60°C. The dielectric and electrical parameters of the PNC films have been analyzed in regards to their suitability as flexible-type novel nanodielectric material for the electrical insulation, the dielectric substrate in the fabrication of high performance organic microelectronic devices, and also in the preparation of nanocomposite solid polymer electrolytes (NSPEs) for the energy storing devices.

Keywords: Polymernanocomposites, Dielectric properties, Electrical conductivity, Relaxation times, Activation energy, X-ray diffraction

Synthetic polymers and their blends had been recognized as the most suitable flexible-type matrices for the preparation of basic composites, nanocomposites and the advanced functional materials for their high performance technological applications[1-9]. Among the synthetic polymers, poly(vinyl alcohol) (PVA) and poly(ethylene oxide) (PEO) are biodegradable, non-toxic, hydrophilic and water soluble materials which form highly flexible-type films when prepared by solution-cast method[10-14]. The high optical transparency of PVA film in the visible region which makes it most suitable as binder for the preparation of various optoelectronic materials[15-17], whereas, the PEO has high solvating power for the alkali metal salts, and therefore, this linear chain polymer has been recognized as the most suitable polymer matrix for the preparation of solid polymer electrolyte (SPE) films[18-20]. The hydroxyl groups and the ether oxygen atoms in the PVA and PEO backbones, respectively, act as functional groups for these polymers which mostly interact with the various additives and nanofillers and turn the material into high performance composites[14-27].

In the last two decades, intensive research is in progress on the inorganic nanofillers loaded polymer nanocomposite (PNCs) for the advancement of materials science and engineering[7-9,28]. These organic-inorganic composite materials comprise various useful properties of inorganic nanofiller (e.g., mechanical, thermal and chemical stabilities) and also of the organic polymer (e.g., flexibility, processability, ductility, dielectric and electrical). The various physical and electrostatic interactions exhibited between the nanofillers and the functional groups or whole polymer chain results in the tremendous enhancement in useful property of the PNC materials. The dispersion of nanosize alumina (Al_2O_3) particles in the PVA structure[27,29-32] and also in the PEO structure[20,33,34] has received significant interest from both the academic and technological point of views.

In addition to several other applications, the PNCs have been established as flexible-type novel

nanodielectrics for their numerous technological uses[35-42]. In the last few years, the author and co-workers have prepared various kind of PNC materials and characterized their detailed dielectric and electrical properties by employing the dielectric relaxation spectroscopy (DRS)[12-14,26,27,33,43-51] in order to explore their nanodielctric applications. Besides the composites based on pristine PVA and PEO matrices, the PVA-PEO blend based films and their various composites have been the interest of several investigators[43,45,50,52-61]. The result of these studies revealed that the different composition blends of PEO and PVA are little miscible due to insignificant heterogeneous polymers chains interactions. But the presence of different additives significantly promotes the miscibility of PVA–PEO blend due to the formation of complex heterogeneous interactions through the additives/nanofillers[43,45,50,52,56-61].

Recently, the author has investigated the detailed structural, dielectric and electrical properties of silica (SiO_2) filled (PVA-PEO)–*x*wt% SiO_2 films[45] and also the zinc oxide (ZnO) filled (PVA-PEO)–*x*wt% ZnO films[50] for their suitability as flexible-type nanodielectrics and also in the preparation of nanocomposite SPE (NSPE) materials. In continuation of the recent work, in the present study, the dielectric and electrical properties and also the structural relaxation processes in (PVA-PEO)–*x*wt% Al_2O_3 films have been investigated in order to explore their applications as novel flexible-type polymer nanodielectric and also the suitability as potential candidate for the advancement of NSPE materials.

Experimental Section

Material

PVA (M_w = 77×10^3 g mol^{-1}) of the LobaChemie, India, and PEO (M_w = 6×10^5 g mol^{-1}) and Al_2O_3 nanopowder (particle size < 50 nm) of the Sigma-Aldrich, USA, were used for the preparation of PNC films. The PVA–PEO blend matrix (50/50 wt%) dispersed with *x*wt% Al_2O_3 (*x* = 0, 1, 3 and 5 weight of alumina/weight of polymer blend) were prepared by solution-casting method. For each sample, firstly the equal amounts of PVA and PEO were dissolved in deionized water, separately, and subsequently, these polymer solutions were mixed which results in the PVA–PEO blend solution. The required amount of Al_2O_3 for each sample was initially dispersed in the deionized water and after that, it w as added slowly into the polymer blend solution, under continuous magnetic stirring to obtain a homogenous solution of (PVA-PEO)–*x*wt% Al_2O_3. Finally, this solution was cast on to a poly propylene dish and was kept to dry at room temperature which results in a stable and free standing PNC film. The PNC films for the various Al_2O_3 concentrations were prepared by following the same procedure as mentioned above. The thicknesses of (PVA-PEO)–*x*wt% Al_2O_3 films were 0.22, 0.18, 0.18 and 0.21 mm corresponding to *x* = 0, 1, 3 and 5 wt % Al_2O_3 films, respectively. These PNC films were vacuum dried at 40°C for 24 h prior to their measurements.

Measurements

The XRD patterns of Al_2O_3nanopowder and the (PVA–PEO)–*x*wt% Al_2O_3 films were recorded in reflection mode at the scan rate 0.05 degree/s using a PANalytical X′pertPro MPD diffractometer of Cu-Kα radiation operating at 45 kV and 40 mA i.e., 1800 W. The DRS measurements of these PNC films were carried out over the frequency range from 20 Hz to 1 MHz using an Agilent technologies 4284A precision LCR meter equipped with 16451B solid dielectric test fixture. Frequency dependent values of capacitance C_p, resistance R_p and dielectric loss tangent (tanδ = ε″/ε′) of the dielectric test fixture loaded with the PNC film were measured in parallel circuit operation for the evaluation of dielectric and electrical spectra of the film. Prior the sample measurement, the open circuit calibration of the cell was performed to eliminate the effect of stray capacitance of the cell leads. During the DRS measurements, the temperature of the PNC film loaded in the dielectric test fixture was controlled by keeping it into the microprocessor controlled oven. The complex dielectric permittivity ε*(ω), alternating current (ac) electrical conductivity σ*(ω), electric modulus $M^*(\omega)$ and complex impedance $Z^*(\omega)$ spectra of the PNC films were determined using the frequency dependent measured values of C_p, R_p, and tanδ in the following equations;

$$\varepsilon^*(\omega) = \varepsilon' - j\varepsilon''; \ \varepsilon' = \frac{t_g C_p}{\varepsilon_0 A} \text{ and } \varepsilon'' = \varepsilon' \tan\delta \quad \ldots (1)$$

$$\sigma^*(\omega) = \sigma' + j\sigma'' = \omega\varepsilon_0\varepsilon'' + j\omega\varepsilon_0\varepsilon' \quad \ldots (2)$$

$$M^*(\omega) = M' + jM'' = \frac{\varepsilon'}{\varepsilon'^2 + \varepsilon''^2} + j\frac{\varepsilon''}{\varepsilon'^2 + \varepsilon''^2} \quad \ldots (3)$$

$$Z^*(\omega) = Z' - jZ'' = \frac{R_p}{1+(\omega C_p R_p)^2} - j\frac{\omega C_p R_p^2}{1+(\omega C_p R_p)^2} \quad \ldots (4)$$

In the above equations, t_g and A are the thickness and the surface area of the PNC film, $\omega = 2\pi f$ is the angular frequency of the applied alternating current electric field and $\varepsilon_0 = 8.85$ pF/m is the dielectric permittivity of vacuum.

Results and Discussion

Structural analysis

The XRD patterns of Al_2O_3nanopowder and PEO, PVA, PVA-PEO blend and (PVA-PEO)–*x*wt% Al_2O_3 films are depicted in Fig 1. The observed diffraction peaks positions and their intensities in the XRD pattern of the Al_2O_3nanopowder were found in agreement with the characteristic diffraction peaks of its γ-phase[33,62,63]. The XRD patterns of pristine PEO and PVA films exhibit the characteristic diffraction peaks (2θ = 19.22° and 23.41° for PEO and 19.59° for PVA) which confirm their semicrystalline structures[64]. The XRD pattern of the pristine PVA–PEO blend film (i.e., at $x = 0$) also exhibit diffraction peaks at 2θ = 19.54° and 23. 66° whichare of nearly equal intensities and are in good agreement with the diffraction peaks of pristine PEO confirming the presence of PEO crystallites in the blend. But the intensity values of both these peaks of PVA–PEO blend are very low as compared to that of the pristine PEO which reveals that the PEO crystalline phase greatly reduces when it is blended with the PVA in equal weight amounts.

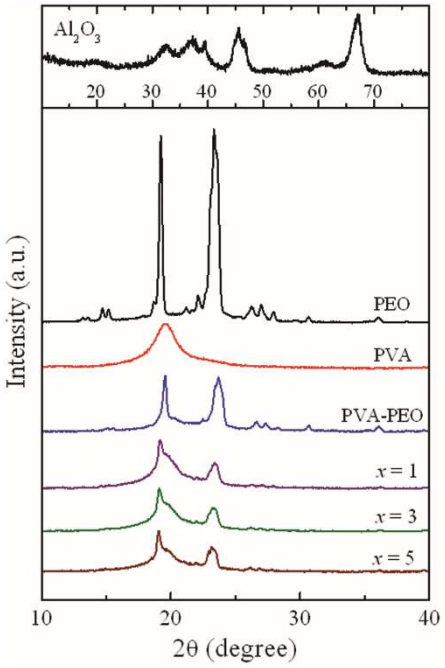

Fig. 1 — XRD patterns of Al_2O_3nanopowder, pristine PEO film, PVA film and (PVA–PEO)–*x*wt% Al_2O_3 polymer nanocomposite films ($x = 0$, 1, 3 and 5) at room temperature

From Fig. 1, it can be noted that the intensities of diffraction peaks of the PVA–PEO blend greatly decrease with the dispersion of only 1 wt% Al_2O_3 in the blend matrix which is attributed to a large decrease in the amount of crystalline phase of the PNC film. Further, it is found that the lower angle peak becomes much boarder, whereas, the decrease in intensity of higher angle diffraction peak is relatively high. This finding also confirms that the PEO crystallite planes have almost deformed in the presence of 1 wt% Al_2O_3 nanoparticles in the PVA–PEO blend. From the figure, it can be noted that the further increase of Al_2O_3 contents in these PNC films (i.e., $x = 3$ and 5 wt%) gradually reduces the crystallinity of the PNC materials. The large decrease of the crystalline phase of the Al_2O_3 loaded PNC films confirms the suitability of these materials in the preparation of nanocomposite solid polymer electrolytes (NSPEs) because the high amorphous phase favours the fast transportation of ions in the host polymer matrix[18,57,60].

Alumina concentration dependent dielectric behaviour

Dielectric spectra

Figure 2 shows the spectra of the real ε′ and loss ε″ parts of the complex dielectric permittivity ε*(ω) and also the dielectric loss tangent (tanδ = ε″/ε′) for the (PVA-PEO)–*x*wt% Al_2O_3nanocomposites at 27°C. The ε′ values of these dielectric materials represent their electrical energy storing ability, whereas the ε″ values attribute to the electric energy loss per cycle through Joule heating effect in these materials. From the ε′ spectra, it can be noted that the ε′ values decrease non-linearly with the increase in frequency from 20 Hz to 1 MHz, which is a common characteristic of the PNC dielectric materials[12–14,26,27,33,43-51]. In comparison to high frequencies ε′ values, the relatively high values of ε′ at low frequencies for these PNC films are due to contribution of interfacial polarization (IP) effect which occurs by the accumulation of charges at the interfaces of different conductivity constituents in these materials under slow varying ac electrical field. The ε″ andtanδ spectra exhibit the relaxation peaks in the intermediate frequency range which are attributed to the cooperative chains segmental dynamics of PVA and PEO in these PNC films. Further, as compared to the ε″ peaks, the tanδ relaxation peaks are relatively intense and clearly distinguishable for these PNC materials. Similar relaxation process was

also observed for the SiO_2 and ZnO loaded PVA–PEO blend based PNC films[45,50].

The values of polymer chain segmental dynamics relaxation time τ_s for these PNC films were determined from the relation $\tau_s = (2\pi f_p)^{-1}$, where $f_p$denotes the frequency value corresponding to the relaxation peak in the tanδ spectra. The observed τ_s values for these PNC films are given in Table 1, which shows that the τ_s values of the Al_2O_3 loaded PNC films are lower than that of the pristine PVA-PEO film. This finding confirms that the cooperative chain segmental dynamics of these polymers enhances in the presence of Al_2O_3 nanoparticles in their structures. The enhancement of polymer chain segmental dynamics favours the suitability of these PNC matrices in the preparation of NSPEsbecause, in the NSPE and SPE materials, the ion transportation occurs coupled with polymer chain segmental dynamics[18-20]. Further, Table 1 shows that the τ_s values of these PNCs vary anomalously with the increase of Al_2O_3 contents in the PVA-PEO blend matrix.

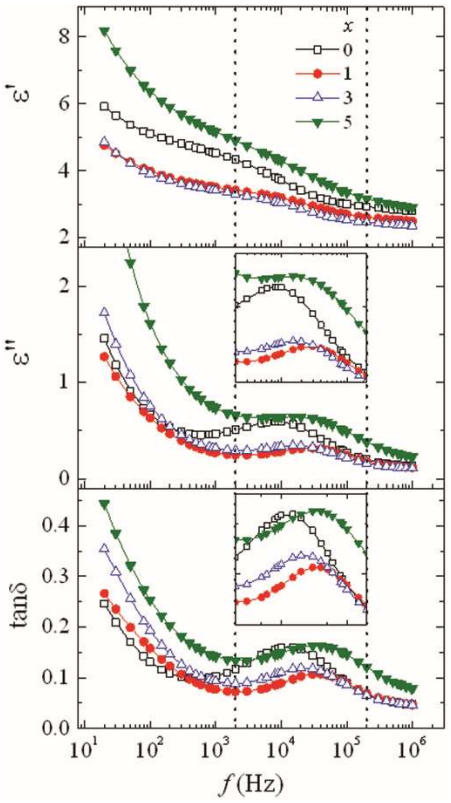

Fig. 2 — Frequency dependent real part ε′ and loss part ε″ of complex dielectric permittivity, and loss tangent tanδ of (PVA–PEO)–*x*wt% Al_2O_3 polymer nanocomposite films (*x* = 0, 1, 3 and 5) at 27°C. Insets show the enlarged view of the spectra over the frequency range 2 kHz–200 kHz

The variation of ε′ values with the increase of Al_2O_3 contents in these PNC films at various fixed frequencies is shown in Fig. 3. From the figure, it can be seen that there is a significant decrease of ε′ values when only 1 wt% Al_2O_3 was dispersed in the PVA-PEO blend matrix, and above that, there is a further small decrease in the ε′ values at 3 wt% Al_2O_3. But for the 5 wt% Al_2O_3 containing PNC films, the ε′ values increase largely and become significantly higher than the corresponding ε′ values of the pristine PVA-PEO blend film at all the frequencies of measurements. The ambient temperature ε′ value of Al_2O_3 nanopowder[31] is 9.7 at 1 MHz, which is about four times high in comparison to that of the pristine PVA-PVP blend film at same frequency and temperature. Besides this fact, the decrease of ε′ values for the 1 and 3 wt% Al_2O_3 containing PNC films as compared to the PVA-PEO blend is mainly due to nanoconfinement effect which occurs when the added inorganic nanoparticles are well separated and homogeneously distributed over the entire volume of the polymer matrix[14,33,36,50,66]. Further the variation of

Table 1 — Values of complex dielectric permittivity $\varepsilon^*(\omega) = \varepsilon' - j\varepsilon''$ at 1 MHz, complex impedance $Z^*(\omega) = Z' - jZ''$ at 20 Hz, polymer chain segmental relaxation time τ_s, electric modulus relaxation time τ_M, dc ionic conductivityσ_{dc} and fractional exponent*n* of the (PVA–PEO)–*x*wt% Al_2O_3 films with the variation of Al_2O_3 concentration (*x*wt%) at 27 °C, and also for the (PVA–PEO)–3 wt% Al_2O_3 PNC film with temperature variation

PNC films	$\varepsilon' - j\varepsilon''$	$Z' - jZ''$ (MΩ)	τ_s (μs)	τ_M (μs)	σ_{dc} (10^{-11} S/cm)	*n*
x (wt%)		(PVA–PEO)–*x*wt% Al_2O_3 films				
0	2.80-*j* 0.13	6.88-*j* 29.50	11.0	8.3	1.33	0.80
1	2.49-*j* 0.12	7.72-*j* 28.32	4.5	3.5	1.86	0.94
3	2.35-*j* 0.11	8.91-*j* 26.31	7.4	5.2	2.06	0.92
5	2.90-*j* 0.23	7.75-*j* 17.92	4.5	2.8	4.19	0.92
T (°C)		(PVA–PEO)–3 wt% Al_2O_3 film				
27	2.35-*j* 0.11	8.91-*j* 26.31	7.4	5.2	2.06	0.92
40	2.38-*j* 0.11	9.69-*j* 22.76	7.3	5.1	2.71	0.84
50	2.41-*j* 0.11	10.19-*j* 17.84	7.1	4.7	3.80	0.76
60	2.46-*j* 0.11	9.41-*j* 10.41	6.8	4.5	7.08	0.65

ε′ values with filler concentration for these (PVA-PEO)–*x*wt% Al_2O_3 films is found identical to that of the (PVA-PEO)–*x*wt% ZnO films[50]. The ε′ – *j*ε″ values of these PNC films at 1 MHz are recorded in Table 1. At 1 MHz, the ε′ values of these PNC films are less than 3 confirming their suitability as polymer nanodielectric of low dielectric permittivity values.

Electric modulus spectra

The real *M′* and imaginary *M″* parts of the complex electric modulus spectra *M**(ω) for (PVA-PEO)–*x*wt% Al_2O_3 nanocomposite films, at 27°C, are depicted in Fig. 4. This figure shows that *M′* values of these PNC materials non-linearly increase with the increase of frequency, whereas, the *M″* spectra exhibit electric modulus relaxation peaks in the frequency range of 10 kHz to 1 MHz. These relaxation peaks also represent the polymer chain segmental motion whichis discussed in the analysis of tanδ spectra of the PNC films. Further, in comparison to the values of tanδ peaks frequency, the *M″* peaks were observed relatively at higher frequencies but their variation with Al_2O_3 contents in the *M″* spectra of the films were found in the same manner as that in the tanδ spectra. Further, the low frequency shapes of the *M″* spectra of these PNC films reflect that there are relaxation peaks just below 20 Hz which can be attributed to the Maxwell-Wagner-Sillars (MWS) polarization process. The shapes of these *M″* spectra and the relaxation processes for the (PVA-PEO)–*x*wt% Al_2O_3 films are found to be in good agreement with that of the (PVA-PEO)–*x*wt% ZnO films[50].

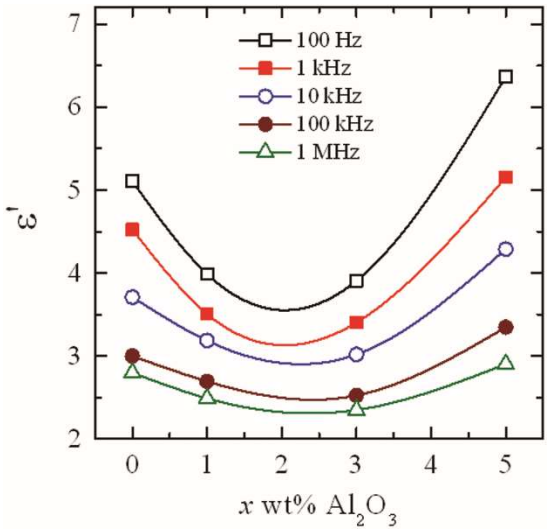

Fig. 3 — Al_2O_3 concentration dependent values of real part ε′ of complex dielectric permittivity for the (PVA–PEO)–*x*wt% Al_2O_3 polymer nanocomposite films at 27°C

The values of electric modulus relaxation time τ_M for the PNC materials were determined from their respective *M″* peak frequency ($f_{p(M)}$) values using the relation $\tau_M = (2\pi f_{p(M)})^{-1}$, and the obtained τ_M values as a function of Al_2O_3 contents in the films are recorded in Table 1. The variation of τ_s and τ_M values with *x*wt% Al_2O_3 for these PNC films is shown in Fig. 5. This figure shows that both the τ_s and τ_M values varies uniformly in the same pattern with the Al_2O_3 contents and the τ_s values remain always higher than the τ_M values, which is a common characteristic observed in various PNC materials[14,33,43,50]. Further, the order of magnitude of these relaxation times of Al_2O_3 containing PVA-PEO films is found in consistent of the relaxation times of SiO_2 and ZnO containing PVA-PEO blend based PNC films[45,50].

Electrical conductivity and impedance spectra

The spectra of real σ′ and imaginary σ″ parts of the complex ac electrical conductivity σ*(ω), and the resistive *Z′* and capacitive reactance *Z″* parts of the complex impedance *Z**(ω) for the (PVA-PEO)–*x*wt% Al_2O_3 films, at 27°C, are shown in Fig. 6. From the figure, it can be noted that, on a log-log scale, the σ′

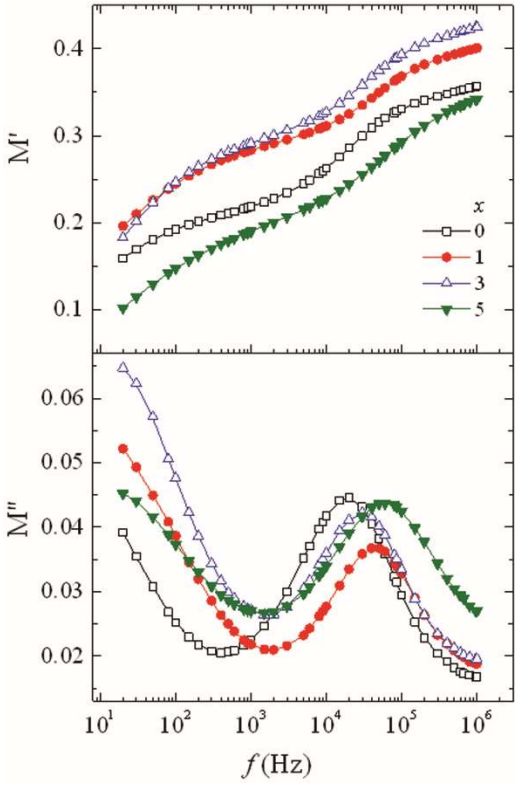

Fig. 4 — Frequency dependent real part *M′* and loss part *M″* of complex electric modulus of (PVA–PEO)–*x*wt% Al_2O_3 polymer nanocomposite films (*x* = 0, 1, 3 and 5) at 27°C

and Z' values of these materials vary non-linearly, whereas the σ″ and Z'' values exhibit linear behaviour with the increase of frequency from 20 Hz to 1 MHz. Further, the σ′ and Z' values are found lower than that of the corresponding σ″ and Z'' values for these (PVA-PEO)–*x*wt% Al_2O_3 films. Furthermore, it can be noted from the figure that the change in σ″ values with Al_2O_3 concentration is relatively low and anomalous, whereas, the σ′ values gradually enhance with the increase of Al_2O_3 contents up to 5 wt% in the PNC film.

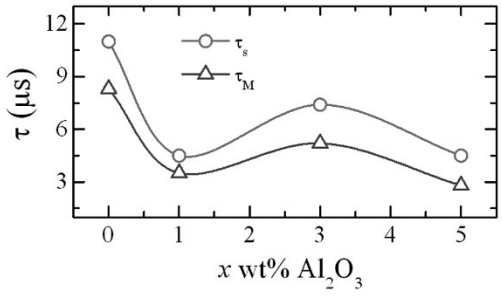

Fig. 5 — Al_2O_3 concentration dependent relaxation times of (PVA–PEO)–*x*wt% Al_2O_3 polymer nanocomposite films at 27°C

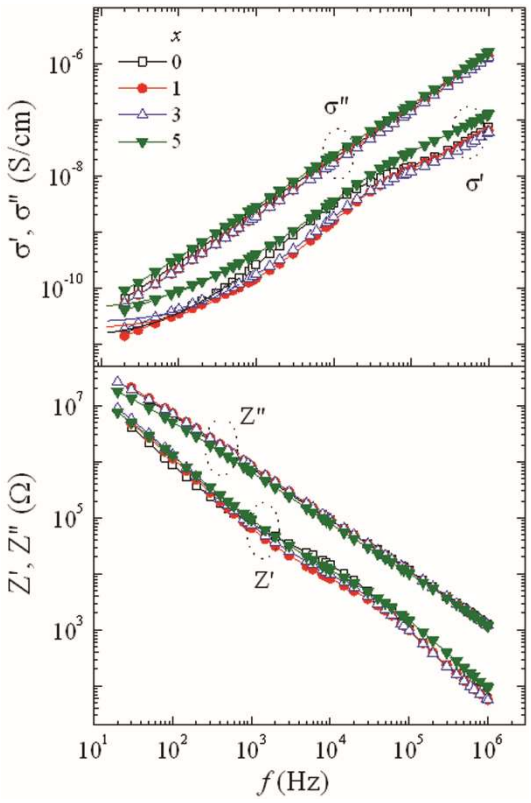

Fig. 6 — Frequency dependent real part σ′ and loss part σ″ of complex ac electrical conductivity, and also the real part Z' and reactive part Z'' of complex impedance of (PVA–PEO)–*x*wt% Al_2O_3 polymer nanocomposite films (*x* = 0, 1, 3 and 5) at 27°C

The direct current (dc) electrical conductivity σ_{dc} values of these PNC films were determined by power law $\sigma'(\omega) = \sigma_{dc} + A\omega^n$ fit of $\sigma'(\omega)$ spectra, where *A* and *n* are pre-exponential factor and fractional exponent, respectively. The σ_{dc} and *n* values obtained from the power law fit of low frequency σ′ values (f< 10 kHz) are recorded in Table 1. The σ_{dc} values for the (PVA–PEO)–*x*wt% Al_2O_3 films are found in the order of 10^{-11} S/cm at ambient temperature and these values non-linearly increase with the increase of Al_2O_3 contents. The *n* values for all the PNC films were found less than unity (Table 1). The $Z^*(\omega)$ values of these PNC films are very high i.e., about 10 MΩ order at 20 Hz (Table 1). The very low values of σ_{dc} and high values of $Z^*(\omega)$ at low frequencies for these PNC materials confirm their suitability as flexible-type nanodielectric materials for electrical insulator and the dielectric substrate which is used in the design and fabrication of the microelectronic devices especially as gate insulator in the field effect transistor.

Temperature dependent dielectric behaviour

The (PVA-PEO)–3 wt% Al_2O_3 film has been studied with temperature variation and its isothermal ε′, ε″ and tanδ spectra are depicted in Fig. 7. From the figure, it can be seen that both the ε′ and ε″ values increase with the increase of temperature of the PNC film which confirms its thermally stimulated dielectric polarization behaviour over the experimental temperature range 27-60°C. Further, the rate of increase of ε′ values with the increase of temperature has increased as the frequency of measuring electric field decreases. The increase of temperature enhances free volume in the composite polymer matrix which favours the dipolar reorientation and their ordering due to which the ε′ values of the PNC film increase[33,45,49,50,64]. The inset of the figure shows the enlarged view of the ε″ andtanδ relaxation peaks which are exhibited in the frequency range of 10 kHz to 100 kHz. The magnitude of the relaxation peaks enhances and these peaks positions have a gradual shift towards higher frequency side with the increase of temperature of the PNC film. The temperature dependent τ_s values for the PNC film were determined using the frequency values corresponding to the peaks and these are given in Table 1. The increase of τ_s values with the increase of temperature of the PNC film reveals that the polymers cooperative chain segmental dynamics increases.

The temperature dependent ε′ values of the (PVA-PEO)–3 wt% Al_2O_3 film, at some selective frequencies viz., 100 Hz, 1 kHz, 10 kHz, 100 kHz and 1 MHz, are shown in Fig. 8. It is observed that the ε′ values increase linearly at radio frequencies, whereas, at lower audio frequencies, these values exhibit non-linearbehaviour with the increase in temperature of the film. Further, Table 1 shows that the increase in ε′ values with the increase of temperature for the higher radio frequency electric field e.g. at 1 MHz, is very low which confirms that this investigated PNC material has almost thermally stable value of its dielectric permittivity (ε′ ~ 2.4 at 1 MHz) over the temperature range 27-60°C. Further, at audio frequencies, the non-linear increase of ε′ values of the PNC film with the increase of temperature reveals that such dielectric materials can also be used as thermally tunable non-linear nanodielectric.

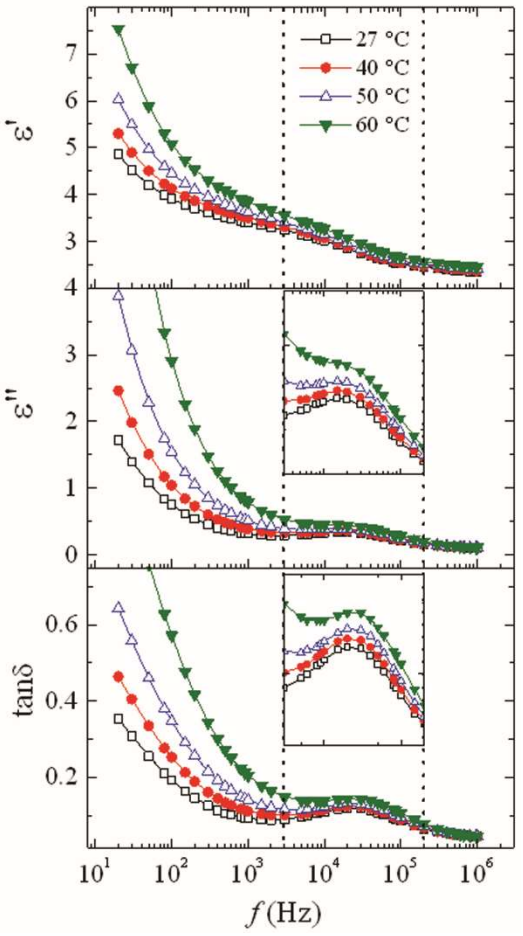

Fig. 7 — Frequency dependent real part ε′ and loss part ε″ of complex dielectric permittivity, and dielectric loss tangent tanδ of (PVA–PEO)–3wt% Al_2O_3 polymer nanocomposite film at different temperatures. Insets show the enlarged view of the spectra over the frequency range 3 kHz–200 kHz

Figure 9 shows the temperature dependent M' and M'' spectra of the (PVA–PEO)–3 wt% Al_2O_3 film. This figure reveals that the M' values have a decrease with the increase of temperature of the PNC film, whereas, the magnitude of relaxation peak of the M'' spectra increases and also has a gradual shift towards higher frequency side. The temperature dependent values of electric modulus relaxation time τ_M for the PNC film were determined from the M'' peak frequency values and these are recorded in Table 1 which decrease with the increase of film temperature. In addition to the polymer chain segmental motion relaxation process observed in the intermediate frequency region, the M'' spectra also exhibit the relaxation peaks around the low frequency end of the spectra at higher temperatures i.e., 50 and 60°C which are attributed to the MWS relaxation process. The shapes of these isothermal M''spectra of the PNC film reveal that the MWS relaxation peak may be around 20 Hz at 40°C, whereas, it is below 20 Hz at 27°C. Further, it is found that the values of MWS relaxation peaks amplitudes are relatively high as compared to the amplitudes of polymer chain segmental relaxation peaks. This result suggests that the MWS relaxation process is more pronounced and sensitive to the temperature of the PNC film in comparison to the chain segmental relaxation process.

Figure 10 depicts the σ′ spectra of (PVA-PEO)–3wt% Al_2O_3 film at various temperatures. The σ′ spectra of the PNC film over the low frequency (f< 10 kHz) range obey the power law relation at all the temperatures which are shown by the solid lines in the figure. The observed temperature dependent values of σ_{dc} and n for the PNC film are recorded in Table 1.

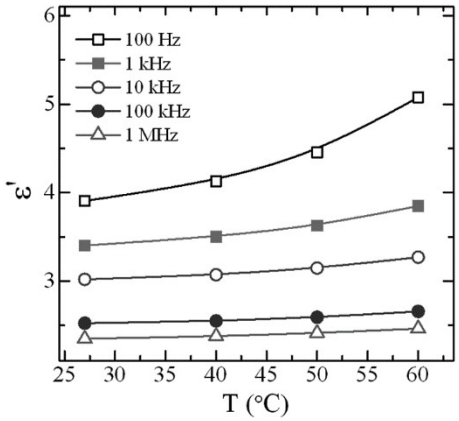

Fig. 8 — Temperature dependent real part ε′ values of complex dielectric permittivity of (PVA–PEO)–3 wt% Al_2O_3 polymer nanocomposite film at various frequencies

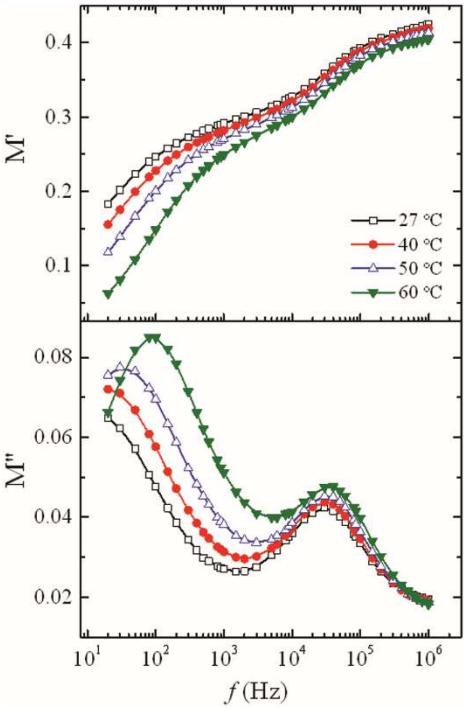

Fig. 9 — Frequency dependent real part M' and loss part M'' of complex electric modulus of (PVA–PEO)–3 wt% Al_2O_3 polymer nanocomposite film at different temperatures

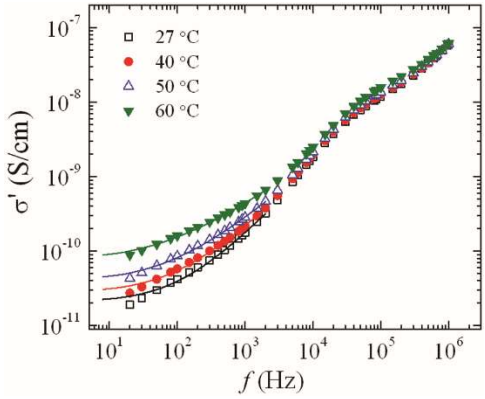

Fig. 10 — Frequency dependent real part σ′ of complex ac electrical conductivity of (PVA–PEO)–3wt% Al_2O_3 polymer nanocomposite film at different temperatures. Solid lines show the power law fit of experimental data in the lower frequency range

It is found that the σ_{dc} values increase whereas n values decrease with the increase of temperature of the PNC film. The n values are lower than unity and these decrease with increase in temperature which confirms that the hopping mechanism of charge transportation becomes stronger as the temperature of the film enhances.

The Arrhenius behaviour of the τ_s, τ_M and σ_{dc} values of the (PVA-PEO)–3 wt% Al_2O_3 film is shown in the Fig. 11. The values of relaxation time activation

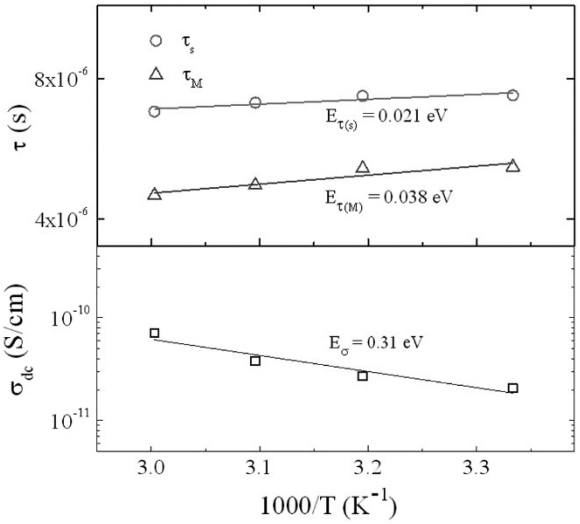

Fig. 11 — Arrhenius behaviour of relaxation times τ_s and τ_M, and dc electrical conductivity σ_{dc} of (PVA–PEO)–3 wt% Al_2O_3 polymer nanocomposite film

energy E_τ and the conductivity activation energy E_σ were determined from the slopes of the Arrhenius plots using the following respective relations;

$$\tau = \tau_0 \exp(E_\tau / k_B T) \quad \ldots (5)$$

$$\sigma_{dc} = \sigma_0 \exp(-E_\sigma / k_B T) \quad \ldots (6)$$

Where, τ_0 and σ_0 are the pre-exponential factors, k_B is the Boltzmann's constant and T is the temperature in absolute scale. The observed E_τ and E_σ values for the PNC film are marked in the figure. The observed E_τ values corresponding to both the relaxation times are found one order of magnitude lower than that of the E_σ values for the PNC film. The very low value of E_τ and also the low value of E_σ confirm that the studied PNC materials are suitable for the preparation of NSPE films with the addition of alkali metal salt because in the low E_τ and E_σ values matrices, the ion transportation occurs relatively fast[20].

Conclusion

The dielectric and electrical properties, and the structural relaxation processes in the (PVA-PEO)–$x$wt% Al_2O_3 films over the frequency range from 20 Hz to 1 MHz are reported. Results reveal that the dispersion of 1 and 3 wt% Al_2O_3 nanoparticles in the PVA–PEO blend matrix significantly lowers the value of dielectric permittivity, whereas, loading of 5 wt% Al_2O_3 in the blend film increases the dielectric permittivity significantly higher than that of

the pristine polymer blend film. The cooperative chain segmental dynamics of the PVA and PEO in the PNC films greatly enhances in the presence of Al_2O_3 nanoparticles in their composite structures. The temperature dependent relaxation times and the dc electrical conductivity values of the PNC film obey the Arrhenius behaviour.

The results of this work confirm that the 1 and 3 wt% Al_2O_3 containing PNC films can be used as low dielectric permittivity value substrate material for the design and development of radio frequency operated microelectronic devices i.e., organic field effect transistors. The temperature dependent dielectric permittivity values of the PNC film exhibit non-linear behaviour at lower audio frequencies, whereas it shows a linear variation at radio frequencies. The very low dc electrical conductivity (10^{-11} S/cm) and the high impedance (~ 10 MΩ) values of these (PVA-PEO)–*x*wt% Al_2O_3 film confirms their suitability as electrical insulator in the preparation of various conventional electronic and electrical devices. The crystalline phase of the PVA-PEO blend matrix greatly reduces on the addition of 1 wt% Al_2O_3 in the blend matrix. The relatively fast polymer chain segmental dynamics and the enhanced amorphous phase infer that these PNC materials can be the potential candidate in the preparation of NSPEs for energy storage device applications.

References

1 Saldivar-Guerra E & Vivaldo-Lima E, *Handbook of Polymer Synthesis, Characterization, and Processing*, (John Wiley & Sons, New Jersey), 2013.
2 Ghosh P, *Polymer Science and Technology*, (McGraw-Hill Education, New York, USA), 2011.
3 Haghi A K, Castro E A, Thomas S, Sivakumar P M & Mercader A G, *Materials Science of Polymers*, (CRC Press, Taylor & Francis Group, Boca Raton, Florida, USA), 2015.
4 Isayev A I, *Encyclopedia of Polymer Blends*, (Wiley-VCH, Weinheim, Germany), 2013.
5 Utracki L A & Wilkie C, *Polymer Blend Handbook*, (Springer, Dordrecht, The Netherlands), 2014.
6 Thomas S, Grohens Y & Jyotishkumar P, *Characterization of Polymer Blends: Miscibility, Morphology and Interfaces*, (Wiley-VCH Verlag GmbH & Co. KGaA, Weinheim, Germany), 2015.
7 Ray S R & Bousmina M, *Polymer Nanocomposites and Their Applications*, (American Scientific Publishers, California, USA), 2008.
8 Gupta R K, Kennel E & Kim K J, *Polymer Nanocomposites Handbook*, (CRC Press, Taylor & Francis Group, Boca Raton, Florida, USA), 2009.
9 Mittal V, *Characterization Techniques for Polymer Nanocomposites*, (Wiley-VCH Verlag GmbH & Co KgaA, Weinheim, Germany), 2012.
10 Van Etten E A, Ximenes E S, Tarasconi L T, Garcia I T S, Forte M M C & Boudinov H, *Thin Solid Films*, 568 (2014)111.
11 Deshmukh K, Ahamed M B, Deshmukh R R, Pasha S K K, Sadasivuni K K, Ponnamma D & Chidambaram K, *EurPolym J*, 76 (2016) 14.
12 Choudhary S & Sengwa R J, *Express Polym Lett*, 4 (2010) 559.
13 Sengwa R J & Choudhary S, *Bull Mater Sci*, 35 (2012) 19.
14 Choudhary S & Sengwa R J, *J Polym Res*, 24 (2017) 54.
15 Im Y M, Oh T H, Nathanael J A & Jang S S, *Mater Lett*, 147 (2015) 20.
16 Tamgadge Y S, Sunatkari A L, Talwatkar S S, Pahurkar V G & Muley G G, *Opt Mater*, 51 (2016) 175.
17 Karthikeyan B, Pandiyarajan T & Mangalaraja R V, *Spectrochim Acta Part A*, 152 (2016) 485.
18 Choudhary S & Sengwa R J, *Mater Chem Phys*, 142 (2013) 172.
19 Sengwa R J & Choudhary S, *Indian J Phys*, 88 (2014) 461.
20 Choudhary S & Sengwa R J, *Electrochim Acta*, 247 (2017) 924.
21 Chandrakala H N, Ramaraj B, Shivakumaraiah, Lee J H &Siddaramaiah, *J Alloys Compd*, 580 (2013) 392.
22 Rao J K, Raizada A, Ganguly D, Ganguly M M, Mankad M M, Satyanarayana S V & Madhu G M, *Polym Bull*, 72 (2015) 2033.
23 Rao J K, Raizada A, Ganguly D, Mankad M M, Satayanarayana S V & Madhu G M, *J Mater Sci*, 50 (2015)7064.
24 Sathish S, Shekar B C & Bhavyasree B T, *Adv Mater Res*, 678 (2013) 335.
25 Joshi G M, Khatake S M, Kaleemula S, Rao N M & Cuberes T, *Curr Appl Phys*, 11 (2011) 1322.
26 Choudhary S &Sengwa R J, *Adv Mat Proc*, 2 (2017) 315.
27 Sengwa R J &Choudhary S, *Adv Mat Proc*, 2 (2017) 280.
28 Zaikov G E, Bazylyak L I, & Haghi A K, *Functional Polymer Blends and Nanocomposites*, (CRC Press, Taylor & Francis Group), 2014.
29 Chibowski S, Paszkiewicz M & Krupa M, *Powder Tech*, 107 (2000) 251.
30 Sonmez M, Ficai D, Stan A, Bleotu C, Matei L, Ficai A & Andronescu E, *Mater Lett*, 74 (2012) 132.
31 Mallakpour S & Khadem E, *Prog Polym Sci*, 51 (2015) 74.
32 Sugumaran S, Bellan C S & Nadimuthu M, *Iran Polym J*, 24 (2015) 63.
33 Sengwa R J & Choudhary S, *J Alloys Compd*, 701 (2017) 652.
34 Das S & Ghosh A, *J Appl Phys*, 117 (2015) 174103.
35 Keith N J, *Dielectric Polymer Nanocomposites*, (Springer Science+Business Media LLC, New York, USA), 2010.
36 Tuncer E, Rondinone A J, Woodward J, Sauers I, James D R & Ellis A R, *Appl Phys A*, 94 (2009) 843.
37 Dang Z M, Yuan J K, Yao S H & Liao R J, *Adv Mater*, 25 (2013) 6334.
38 Qiao Y, Islam M S, Han K, Leonhardt E, Zhang J, Wang Q, Ploehn H J & Tang C, *Adv Funct Mater*, 23 (2013) 5638.
39 Luzio A, Ferré F G, Fonzo F D & Caironi M, *AdvFunct Mater*, 24 (2014) 1790.
40 Y Zhou, J He, J Hu & B Dang, *J Appl Polym Sci*, 133 (2016) 42863.
41 Mansour Sh A, Elsad R A & Izzularab M A, *J Polym Res*, 23 (2016) 1.
42 Anandraj J & Joshi G M, *Compos Interface*, 2017, DOI: 10.1080109276440.2017.1361717.
43 Sengwa R J, Choudhary S & Sankhla S, *Comps Sci Tech*, 70 (2010) 1621.

44 Sengwa R J & Choudhary S, *Macromol Symp*, 362 (2016) 132.
45 Choudhary S, *Indian J Eng Mater Sci*, 23 (2016) 399.
46 Choudhary S & Sengwa R J, *J Appl Polym Sci*, 133 (2016) 44568.
47 Choudhary S & Sengwa R J, *J Appl Polym Sci*, 124 (2012) 4847.
48 Choudhary S & Sengwa R J, *AIP Conf Proc*, 1728 (2016) 020420.
49 Choudhary S, *Comp Comm*, 5 (2017) 54.
50 Choudhary S, *Physica B*, 522 (2017) 48.
51 Choudhary S, *Indian J Chem Technol*, 24 (2017) 311.
52 Mishra R & Rao K J, *Solid State Ionics*, 106 (1998) 113.
53 Lai W C & Liau W B, *J Appl Polym Sci*, 92 (2004) 1562.
54 Paladhi R & Singh R P, *J Appl Polym Sci*, 51 (1994) 1559.
55 Sawatari C & Kondo T, *Macromolecules*, 32 (1999) 1949.
56 Abd El-Kader F H, Hakeem N A, Elashmawi I S & Ismail A M, *Indian J Phys*, 87 (2013) 983.
57 Joge P, Kanchan D K, Sharma P & Gondaliya N, *Indian J Pure Appl Phys*, 51 (2013) 350.
58 Joge P & Kanchan D K, *Adv Mater Res*, 1141 (2016) 19.
59 Joge P, Kanchan D K, Sharma P & Gondaliya N, *Adv Mater Res*, 665 (2013) 227.
60 Joge P N, Kanchan D K & Sharma P L, *AIP Conf Proc*, 1591 (2014) 356.
61 Aziz S B, Abdullah O Gh, Hussein A M, Abdulwahid R T, Rasheed M A, Ahmed H M, Abdalqadir S W & Mohammed A R, *J Mater Sci Mater Electron*, 28 (2017) 7473.
62 Tok A I Y, Boey F Y C & Zhao X L, *J Mater Process Tech*, 178 (2006) 270.
63 Wang Y, Shih K & Jiang X, *Ceram Int*, 38 (2012) 1879.
64 Sengwa R J & Choudhary S, *J Appl Polym Sci*, 131 (2014) 40617.
65 Choudhary S & Sengwa R J, *Polym Bull*, 72 (2015) 2591.
66 Nelson J K & Hu Y, *J Phys D: Appl Phys*, 38 (2005) 213.